

## Problems with using radiocarbon to infer ocean ventilation rates for past and present climates

Jean-Michel Campin<sup>a,\*</sup>, Thierry Fichefet<sup>a</sup>, Jean-Claude Duplessy<sup>b</sup>

<sup>a</sup> Institut d'Astronomie et de Géophysique G. Lemaître, Université catholique de Louvain, 2 Chemin du Cyclotron, B-1348 Louvain-la-Neuve, Belgium

<sup>b</sup> Laboratoire des Sciences du Climat et de l'Environnement, Laboratoire mixte CNRS–CEA, F-91198 Gif sur Yvette cedex, France

Received 10 June 1998; accepted 23 October 1998

---

### Abstract

The oceanic  $^{14}\text{C}$  distribution reflects mainly the circulation pattern and intensity, but is also sensitive to the exchange processes at the air–sea interface. In order to separate the relative contributions of both effects (that might have changed in the past), we incorporate in an ocean general circulation model two passive tracers, namely, the normalized radiocarbon ratio ( $\Delta^{14}\text{C}$ ) and the actual age of water. We quantify, for both present and glacial conditions, the decoupling between the  $^{14}\text{C}$  ventilation rate and the circulation intensity as the difference between the simulated  $^{14}\text{C}$  age and actual age of water. The  $^{14}\text{C}$  age of the model Antarctic Bottom Water (AABW) appears systematically older than its actual age, the discrepancy being larger for glacial conditions because of the more extensive Antarctic sea-ice cover. Our results suggest that the AABW flow rate could have been stronger than today during the Last Glacial Maximum, contrary to what might be inferred from a naive interpretation of  $^{14}\text{C}$  measurements in deep-sea sediment cores. © 1999 Elsevier Science B.V. All rights reserved.

*Keywords:* ocean circulation; models; paleoceanography; last glacial maximum; C-14; air–sea interface

---

### 1. Introduction

Natural radiocarbon concentration in the ocean is an invaluable tool to assess the ventilation rate of the deep water masses, which is closely related to the deep-ocean circulation [1,2]. For instance, the measurements of oceanic  $^{14}\text{C}$  concentration made in the seventies during the Geochemical Ocean Sections Study (GEOSECS) [3,4] support the idea of a conveyor-like circulation, with deep-water  $^{14}\text{C}$  age

increasing gradually from the North Atlantic to the Indian Ocean and the North Pacific, where the oldest deep water is found [1]. However, as the  $\text{CO}_2$  exchange between atmosphere and ocean is globally slow and, above all, largely reduced in ice-covered regions, the deep water formed there may be strongly depleted in  $^{14}\text{C}$  relatively to the atmosphere, especially near Antarctica where the newly formed Antarctic Bottom Water (AABW) has a much lower  $^{14}\text{C}$  content than the newly produced North Atlantic Deep Water (NADW). This induces a decoupling between the  $^{14}\text{C}$  ventilation rate and the circulation intensity [1,5], that might have changed in the past.

---

\* Corresponding author. Tel.: +32 10 473080; Fax: +32 10 474722; E-mail: campin@astr.ucl.ac.be

Here, we investigate this decoupling for present-day and glacial conditions with a global ocean model including two passive tracers, namely, the normalized radiocarbon ratio ( $\Delta^{14}\text{C}$ ) and the actual age of water, which is defined as the time elapsed since the water parcel has left the surface.

## 2. Model, forcing and experimental design

The model used in the present work is a primitive-equation, free-surface ocean general circulation model [6]. To avoid the singularity at the North Pole associated with the geographical spherical coordinates, two spherical grids connected in the equatorial Atlantic are employed: a grid with its poles located on the geographical equator for the North Atlantic and the Arctic, and a classical latitude–longitude grid for the rest of the world ocean [7]. The horizontal resolution is of  $3^\circ \times 3^\circ$ . Vertically there are 15 levels, covering a total depth of 5500 m and expanding in thickness from 20 m at the surface to 700 m at the bottom. The bathymetry represents a discretized version of the real world ocean bottom topography. For this study, two passive tracers are introduced into the model: the  $\Delta^{14}\text{C}$  [8], following the approach of Toggweiler et al. [9], and the actual age of water [10]. We use the acceleration technique of Bryan and Lewis [11] to speed up the model convergence towards equilibrium, which is reached after 2700 yr of integration, or the equivalent 8600 yr at the model bottom level.

Two experiments are performed with the model, both under annual mean restoring boundary conditions: a control run with present-day forcing, and a run with conditions that prevailed during the Last Glacial Maximum (LGM). In the control run, the atmosphere-to-ocean momentum flux is determined from annual mean climatological wind-stress fields [12]. The surface fluxes of heat and fresh water are implied by restoring the temperature and salinity of the model uppermost level to the respective annual mean surface data of Levitus [13]. It should be noted that, a slight salinity correction (+0.4 practical salinity units, psu) is applied over the continental shelves of the Weddell and Ross Seas to mimic the winter brine-release effect that is absent in Levitus' salinities [14]. On the other hand, north of  $60^\circ\text{N}$ , winter

temperatures are used (rather than annual mean values) to better represent winter deep-water formation. The  $^{14}\text{C}$  exchange rate with the atmosphere ( $\Delta^{14}\text{C} = 0$ ) is wind-speed dependent [15], and is reduced proportionally to the sea-ice concentration. Wind speed is evaluated from the wind-stress magnitude. The sea-ice concentration is set equal to 90% in regions of perennial ice, and is assumed to decrease linearly with latitude in the seasonal ice zone. The extents of these zones are taken from CLIMAP [16]. It is worth pointing out that the gas-exchange rate is uniformly adjusted to match the observed global mean value of  $18 \text{ mol (C) m}^{-2} \text{ yr}^{-1}$  [17] (the surface total carbon content is taken as  $2 \text{ mol (C) m}^{-3}$  everywhere [9]).

In the glacial experiment, wind-stress anomalies computed by an atmospheric general circulation model [18] and CLIMAP's [16] annual mean sea-surface temperatures are utilized. As regards the haline forcing, the salinity reconstruction of Duplessy et al. [19] is used in the Atlantic. Elsewhere, because of the lack of salinity data, we employ the modern forcing values enhanced by 1 psu to account for the glacial sea-level reduction. An additional +0.4 psu salinity anomaly is applied in the Weddell and Ross Seas, as suggested by the few available data in the Weddell Sea [20]. The seas shallower than 130 m are removed, and the Bering Strait is closed, in accordance with glacial bathymetry. The glacial  $^{14}\text{C}$  forcing is established in a similar way as in the control run, with the same normalization constant. However, the glacial sea-ice and wind-stress fields are used. Furthermore, the glacial  $p\text{CO}_2$  reduction (200 ppm/280 ppm) is taken into account, but this has almost no impact on the  $^{14}\text{C}$  age considered here, which is relative to the globally averaged surface value (modern: 360 yr; LGM: 610 yr). Regarding the actual age of water, a strong restoring (relaxation time scale of 3 days) towards a zero value is applied at the uppermost level in the two experiments, in both ice-covered and ice-free regions and regardless of surface wind speed.

## 3. Results and discussion

The model successfully reproduces the known large-scale features of the modern ocean circulation. In the Atlantic (Fig. 1a),  $8 \times 10^6 \text{ m}^3 \text{ s}^{-1}$  (8 sver-

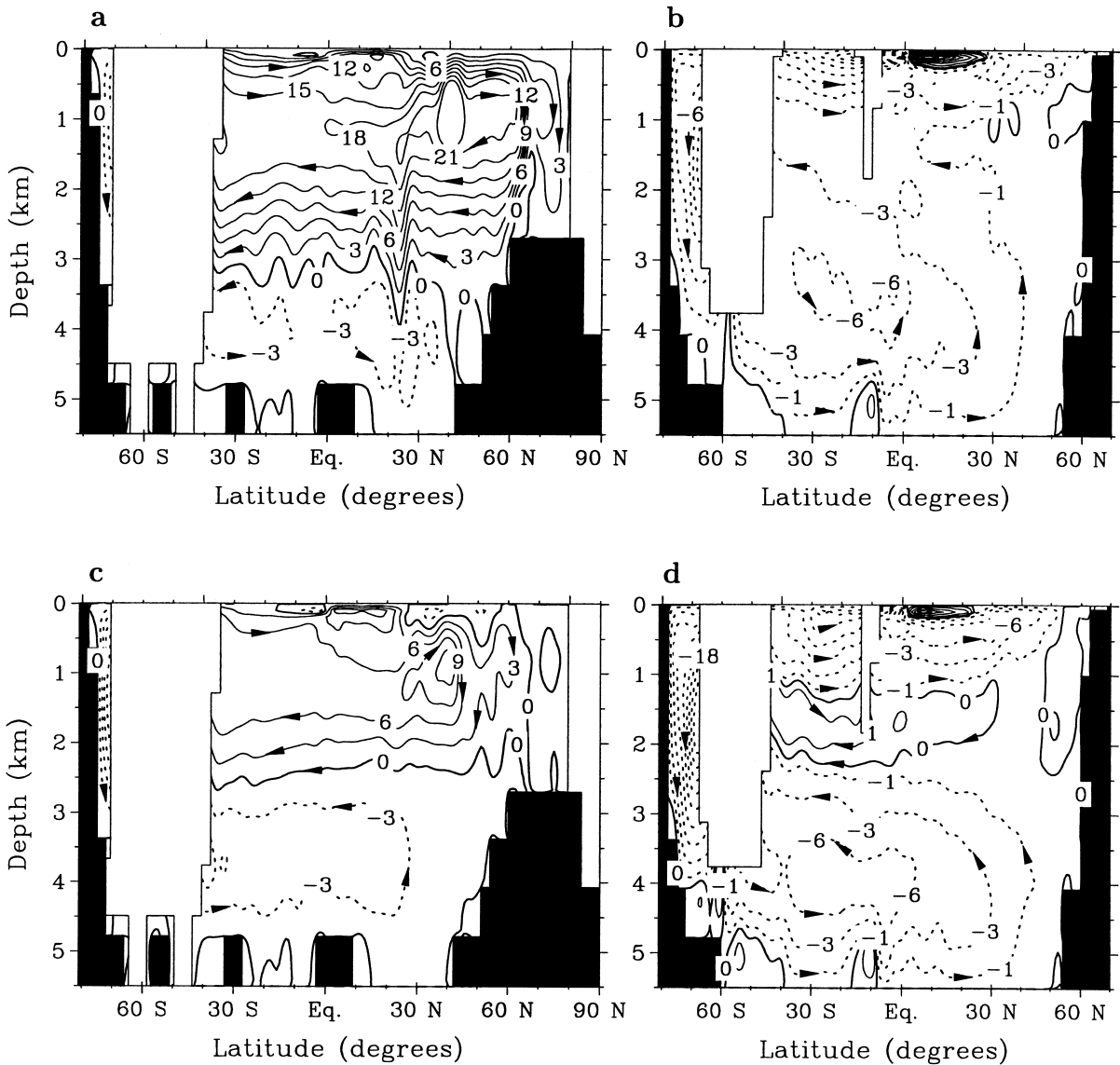


Fig. 1. Contours of the annual mean meridional overturning stream function in the Atlantic and Pacific basins for the control run (a and b, respectively) and the LGM experiment (c and d, respectively). Flow is clockwise around solid contours. Units are Sv (1 sverdrup =  $10^6 \text{ m}^3 \text{ s}^{-1}$ ).

drups (Sv)) of dense water produced in the Nordic Seas sink to great depths south of Greenland and form NADW with an additional supply of less dense water. This water mass flows southwards at depths of 2000–3500 m, and is ultimately exported (17 Sv) to the other basins through the Southern Ocean. A northward flow (4 Sv) of AABW feeds the deepest part of the Atlantic. All these characteristics are con-

sistent with observational estimates [21,22]. Below 3500 m, deep water enters the Pacific basin from the south (Fig. 1b). Only a small amount of this water (~1 Sv) upwells towards the base of the thermocline, the remainder returning to the Southern Ocean at intermediate depths, in qualitative agreement with observations [23].

The distribution of the  $^{14}\text{C}$  age of water derived

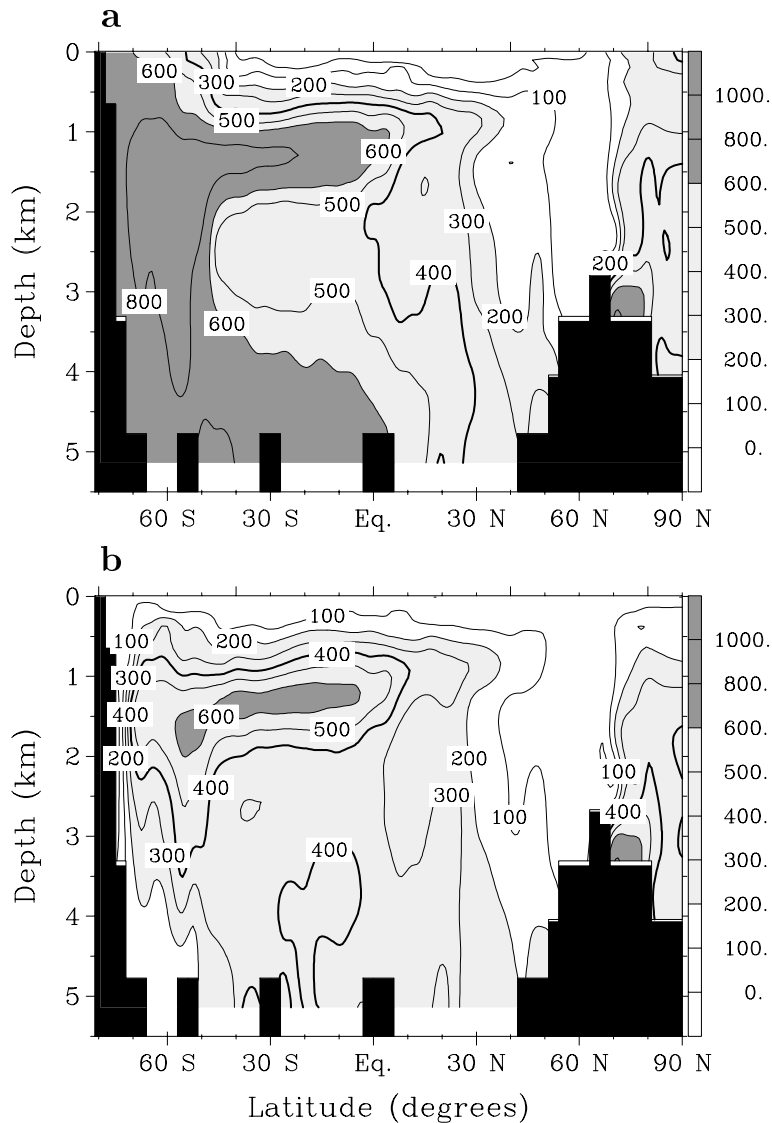


Fig. 2. Latitude–depth distributions of the zonal mean  $^{14}\text{C}$  age (a) and actual age (b) of water in the Atlantic for the control run. Units are yr. The  $^{14}\text{C}$  ages are derived from the simulated  $\Delta^{14}\text{C}$ , and are relative to the globally averaged surface value stemmed from the model (360 yr). Note that the model AABW and AAIW ‘appear’ old in  $^{14}\text{C}$  due to the sea-ice shielding of the air–sea  $^{14}\text{C}$  exchange; this effect is not present in the actual age tracer simulation.

from the model  $\Delta^{14}\text{C}$  reinforces the confidence that we have in the simulated circulation and proves the realism of the  $^{14}\text{C}$  boundary conditions used here. For instance, the 500-yr isoline (corresponding to  $\Delta^{14}\text{C} = -100\text{‰}$ ) in the Atlantic (Fig. 2a) matches rather well the GEOSECS data [3], and clearly separates the core of well-ventilated NADW from the older AABW below and Antarctic Intermediate Wa-

ter (AAIW) above. In the Pacific, the computed  $^{14}\text{C}$  ages (not shown) qualitatively agree with the observations [4]. As in the real ocean, the oldest water is found around 2000 m in the northern part of the basin. However, this water mass appears too depleted in  $^{14}\text{C}$  (by 40‰), which could arise from the fact that the Pacific deep-water circulation is a little too sluggish in the model.

When glacial boundary conditions are imposed, the model produces a circulation in the Atlantic that compares favorably with the reconstructions made from proxy data [24–27] and other models [28–30]. Actually, the sites of deep convection are shifted to 50–55°N, 20–40°W, about midway between North America and Europe. At the same time, the NADW overturning has become shallower and much weaker (only 7 Sv of so-called glacial North Atlantic Intermediate Water (GNAIW) are exported to the other basins), leaving most of the deep Atlantic under the influence of the AABW (Fig. 1c). In the Pacific (Fig. 1d), two thermohaline circulation cells are noticed: a weak clockwise cell centered around 1500 m, which comes with a stronger northward intrusion of AAIW, and below, a slightly strengthened AABW cell. Compared to the control run, the temperature of the deep Atlantic is reduced by approximately 2°C, in accordance with oxygen-isotope estimates [27]. This cooling is primarily caused by the replacement of the relatively warm modern NADW by cold AABW. In the other basins, the deep ocean experiences a more moderate cooling (~1°C).

The reorganization of the ocean thermohaline circulation discussed above leads to major changes in the distribution of the  $^{14}\text{C}$  age of water. Fig. 3a shows younger intermediate water (around 1000 m) and much older deep water (below 2000 m) in the Atlantic, in qualitative agreement with the few  $^{14}\text{C}$  measurements in sediment cores [2]. This results in a strong vertical gradient of  $^{14}\text{C}$  age around 2500 m in the North Atlantic, which separates the old AABW from the newly formed GNAIW. Also of interest is the absence of relatively old intermediate water in the North Atlantic, especially between 25° and 65°N, which contrasts with the modern case. These characteristics are consistent with the water-mass vertical structure derived from  $\delta^{13}\text{C}$  and other proxies [25,26,31,32]. The large age difference found in the deep Norwegian Sea and Arctic Ocean is a consequence of the strong surface stratification there that is imposed by the LGM forcing [16,19]. However, this forcing feature is highly controversial [33]. In an additional LGM experiment, using other sea-surface temperature and salinity reconstructions [33,34] over the Norwegian Sea, the above-mentioned age difference is reduced by more than 60%, whereas the glacial circulation and ventilation rate remain

approximately the same elsewhere. Fig. 3b indicates that the  $^{14}\text{C}$  age of water in the deep part of the Pacific is older than in the control run south of the equator and younger north of it. The latter characteristics is a consequence of the more vigorous bottom circulation and, above all, of the influence at great depths of the inflow of very young AAIW (see Fig. 1d), that is absent in the modern circulation. This ventilation pathway of the deep Pacific confirms the interpretation of  $\delta^{13}\text{C}$  data given by Michel et al. [35].

A significantly different pattern is shown by the actual age of water, which is only function of the circulation intensity, whereas the  $^{14}\text{C}$  age also depends on the rate of  $^{14}\text{C}$  exchange at the air–sea interface. A knowledge of the actual age of water therefore allows to distinguish in a  $\Delta^{14}\text{C}$  signal the ageing effect related to the circulation from the one associated with the surface exchange. For instance, in the modern far southern Atlantic, the  $^{14}\text{C}$  age is roughly uniform and quite old (~700 yr; Fig. 2a), a priori suggesting a rather slow overturning there. On the contrary, the newly produced AABW that originates from the Weddell Sea continental shelf forms a narrow band of very young water (actual age of water <100 yr) close to the Antarctic continent (Fig. 2b), which attests a fast water-mass turnover. In the same way, the actual age of water indicates that the AABW in the low- and mid-latitude South Atlantic is renewed at the same rate as the overlying NADW, while the  $^{14}\text{C}$  age increases with depth.

Two reasons may be invoked to explain the difference between the  $^{14}\text{C}$  and actual ages of the AABW. First, the  $^{14}\text{C}$  exchange at the air–sea interface is globally slow. This low exchange rate does not impact seriously on the newly formed NADW, because the Atlantic surface water has enough time to incorporate atmospheric  $^{14}\text{C}$  during its long northward journey from the subtropical latitudes to the sinking areas. In the Southern Ocean, the strong westerlies that prevail over the northern part of the Antarctic zone are responsible for an intense northward Ekman transport and upwelling of old Circumpolar Deep Water (CDW) at the Antarctic divergence zone (~60°S). South of this divergence zone, surface waters are isolated from the well-ventilated,  $^{14}\text{C}$ -rich subtropical waters. As their surface residence time is short with respect to the air–sea  $^{14}\text{C}$  exchange

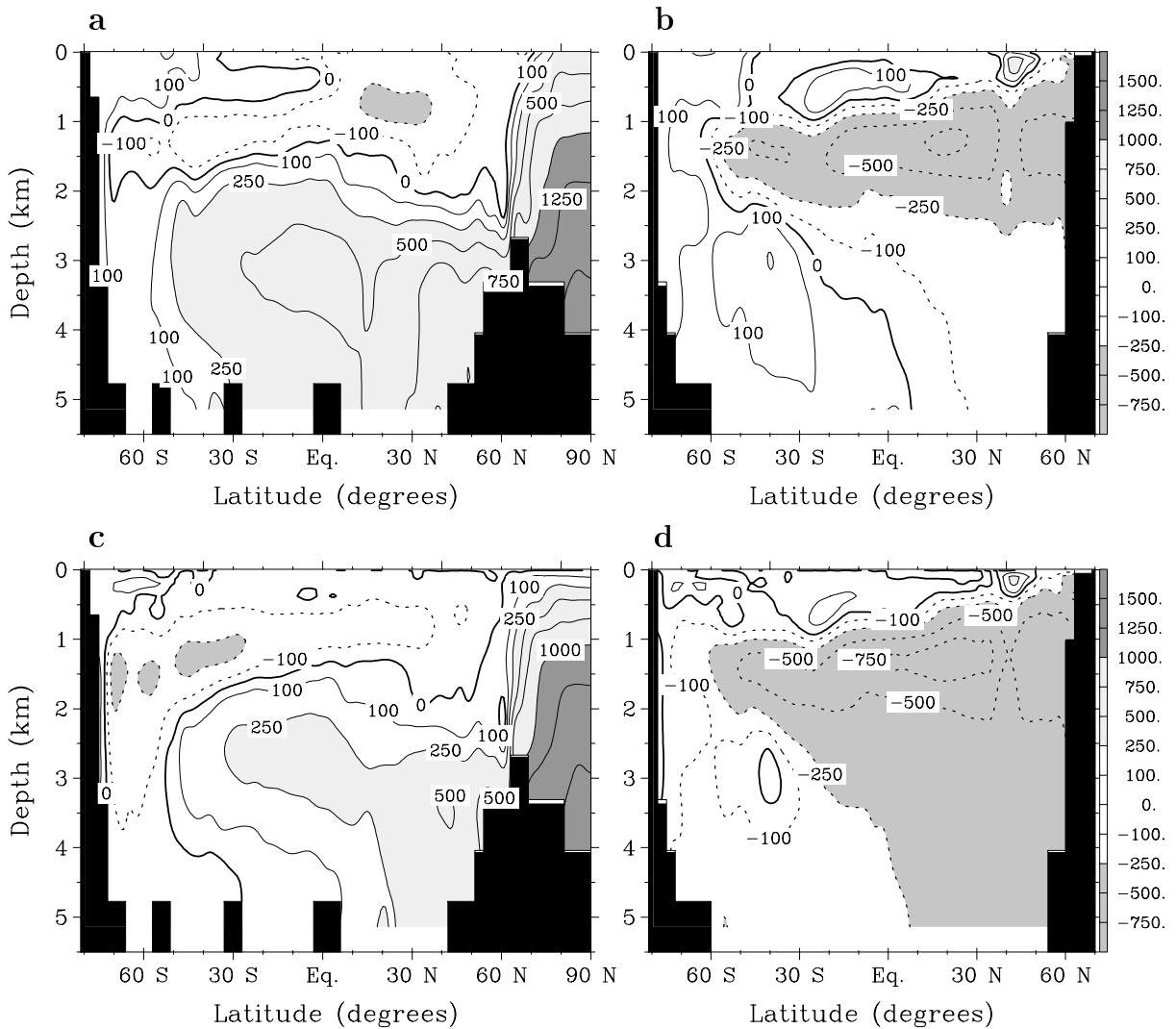


Fig. 3. Latitude–depth distributions of the difference in zonal mean  $^{14}\text{C}$  age between the LGM and control experiments in the Atlantic and in the Pacific (a and b, respectively); difference in actual age of water between the LGM and control experiments in the Atlantic and Pacific (c and d, respectively). Units are yr.

rate, they have not taken up enough  $^{14}\text{C}$  to reach equilibrium with the atmosphere. Second, because of the strong compactness of sea ice and the weakness of the wind over the Weddell and Ross Seas, the  $^{14}\text{C}$  transfer coefficient is small in the regions of AABW formation. Although AABW formation in the model, as in the real ocean [36], involves different water masses (including very young shelf water and old CDW), the age shift at the surface (500–700 yr) is to a large extent transferred to the bottom.

Interestingly, the differences between the  $^{14}\text{C}$  and actual ages of water significantly increase when glacial boundary conditions are used to drive the model. The global mean actual age is 150 yr younger in the LGM simulation compared to the modern one, indicating a global oceanic circulation faster than the present during the LGM. However, the globally averaged  $^{14}\text{C}$  age is roughly the same for the two experiments. At the regional scale, larger differences are observed. As the permanent sea-ice cover around

Antarctica extends northwards beyond the Antarctic divergence in the glacial run, the air–sea exchange of  $^{14}\text{C}$  is drastically reduced in the region where the surface waters contributing to AABW formation reside. This implies a larger age shift at the LGM for the newly produced AABW. As can be seen from Fig. 3, this water has a  $^{14}\text{C}$  age which is about 100 yr older than in the control case, while its actual age is approximately 100 yr younger. On the other hand, the AABW invades a large portion of the glacial deep ocean, especially the deep Atlantic. Since the AABW is the main water mass concerned by the age shift, even in the modern simulation, its larger influence in the glacial ocean yields an enhanced  $^{14}\text{C}$  ageing effect. The combination of the two effects is particularly dramatic below 3000 m in the deep Atlantic, with changes in  $^{14}\text{C}$  age (Fig. 3a) that are systematically greater (by 300 yr) than changes in actual age (Fig. 3c).

Our results reveal that the interpretation of  $^{14}\text{C}$  age may lead to erroneous conclusions regarding circulation changes. For instance, in the glacial run, the deep convection close to Antarctica and the AABW circulation increase in strength (Fig. 1), resulting in actual ages of water at the deepest model levels in the South Pacific that are noticeably younger than in the modern experiment (Fig. 3d). In contrast, the  $^{14}\text{C}$  ages in this zone are slightly older (Fig. 3b), in general agreement with estimates obtained from benthic foraminifera [37].

The processes responsible for the difference in  $^{14}\text{C}$  ventilation rate between the LGM and present time are likely to affect in a similar way the total  $\text{CO}_2$  and  $^{13}\text{C}$  concentrations, although the full carbon cycle has to be considered for these two tracers. So, we infer that these mechanisms could partly explain the very low AABW  $\delta^{13}\text{C}$  values recorded in glacial sediments [38], since the  $^{14}\text{C}$  concentration follows the same tendency.

### Acknowledgements

We thank A. Mouchet for helpful discussions about various aspects of this study. M. England and an anonymous reviewer provided constructive comments that improve the manuscript. This work was supported by the EU (J.M.C. and J.C.D.), the

Belgian FNRS (T.F.), and the French CNRS, CEA, and INSU-PNEDC (J.C.D.). [ACJ]

### References

- [1] M. Stuiver, P.D. Quay, H.G. Östlund, Abyssal water carbon-14 distribution and the age of the world oceans, *Science* 219 (1983) 849–851.
- [2] W.S. Broecker, T.-H. Peng, S. Trumbore, G. Bonani, W. Wolfli, The distribution of radiocarbon in the glacial ocean, *Global Biogeochem. Cycles* 4 (1990) 103–117.
- [3] M. Stuiver, H.G. Östlund, GEOSECS Atlantic radiocarbon, *Radiocarbon* 22 (1980) 1–24.
- [4] H.G. Östlund, M. Stuiver, GEOSECS Pacific radiocarbon, *Radiocarbon* 22 (1980) 25–53.
- [5] W.S. Broecker, A revisited estimate for the radiocarbon age of North Atlantic Deep Water, *J. Geophys. Res.* 84 (1979) 3218–3226.
- [6] E. Deleersnijder, J.-M. Campin, On the computation of the barotropic mode of a free-surface world ocean model, *Ann. Geophys.* 13 (1995) 675–688.
- [7] E. Deleersnijder, J.-P. van Ypersele, J.-M. Campin, An orthogonal, curvilinear coordinate system for a world ocean model, *Ocean Modelling* 100 (unpublished manuscript) (1993) 7–10 (+ figures).
- [8] M. Stuiver, H. Polach, Discussion reporting of  $^{14}\text{C}$  data, *Radiocarbon* 19 (1977) 355–363.
- [9] J.R. Toggweiler, K. Dixon, K. Bryan, Simulations of radiocarbon in a coarse-resolution world ocean model. 1. Steady state prebomb distributions, *J. Geophys. Res.* 94 (1989) 8217–8242.
- [10] M.H. England, The age of water and ventilation timescales in a global ocean model, *J. Phys. Oceanogr.* 25 (1995) 2756–2777.
- [11] K. Bryan, L.J. Lewis, A water mass model of the world ocean, *J. Geophys. Res.* 84 (1979) 2503–2517.
- [12] Y.-J. Han, S.-W. Lee, An analysis of monthly mean wind stress over the global ocean, *Mon. Weather. Rev.* 111 (1983) 1554–1566.
- [13] S. Levitus, Climatological atlas of the world ocean, NOAA Prof. Pap. 13, US Govt Printing Office, Washington DC, 1982, 173 pp.
- [14] M.H. England, Representing the global-scale water masses in ocean general circulation models, *J. Phys. Oceanogr.* 23 (1993) 1523–1552.
- [15] R. Wanninkhof, Relationship between wind speed and gas exchange over the ocean, *J. Geophys. Res.* 97 (1992) 7373–7382.
- [16] CLIMAP Project Members, Seasonal reconstruction of the Earth's surface at the last glacial maximum, Map Chart Ser. MC-36, Geol. Soc. Am., Boulder, 1981.
- [17] U. Siegenthaler, Carbon dioxide: Its natural cycle and anthropogenic perturbation, in: P. Buat-Ménard (Ed.), *The Role of Air–sea Exchange in Geochemical Cycling*, Reidel, Dordrecht, 1986, pp. 209–247.

- [18] M. Lautenschlager, K. Herterich, Atmospheric response to ice age conditions: Climatology near the Earth's surface, *J. Geophys. Res.* 95 (1990) 22547–22557.
- [19] J.-C. Duplessy, L. Labeyrie, A. Juillet-Leclerc, F. Maitre, J. Duprat, M. Sarnthein, Surface salinity reconstruction of the North Atlantic Ocean during the last glacial maximum, *Oceanol. Acta* 14 (1991) 311–324.
- [20] J.-C. Duplessy, L. Labeyrie, M. Paterne, S. Hovine, T. Fichet, J. Duprat, M. Labracherie, High latitude deep water sources during the last glacial maximum and the intensity of the global oceanic circulation, in: G. Wefer, W.H. Berger, G. Siedler, D.J. Webb (Eds.), *The South Atlantic: Present and Past Circulation*, Springer, Berlin, 1996, pp. 445–460.
- [21] R.R. Dickson, J. Brown, The production of North Atlantic Deep Water: Sources, rates, and pathways, *J. Geophys. Res.* 99 (1994) 12319–12341.
- [22] W.J. Schmitz, M.S. Mc Cartney, On the North Atlantic circulation, *Rev. Geophys.* 31 (1993) 29–49.
- [23] W.J. Schmitz, On the interbasin-scale thermohaline circulation, *Rev. Geophys.* 33 (1995) 151–173.
- [24] E.A. Boyle, L.D. Keigwin, North Atlantic thermohaline circulation during the past 20,000 years linked to high-latitude surface temperature, *Nature* 330 (1987) 35–40.
- [25] J.-C. Duplessy, N.J. Shackleton, R.G. Fairbanks, L. Labeyrie, D. Oppo, N. Kallel, Deepwater source variations during the last climatic cycle and their impact on the global deepwater circulation, *Paleoceanography* 3 (1988) 343–360.
- [26] M. Sarnthein, K. Winn, S.J.A. Jung, J.-C. Duplessy, L. Labeyrie, H. Erlenkeuser, G. Ganssen, Changes in east Atlantic deepwater circulation over the last 30,000 years: Eight time slice reconstructions, *Paleoceanography* 9 (1994) 209–267.
- [27] L. Labeyrie, J.-C. Duplessy, J. Duprat, A. Juillet-Leclerc, J. Moyes, E. Michel, N. Kallel, N.J. Shackleton, Changes in the vertical structure of the North Atlantic ocean between glacial and modern times, *Quat. Sci. Rev.* 11 (1992) 401–413.
- [28] T. Fichet, S. Hovine, J.-C. Duplessy, A model study of the Atlantic thermohaline circulation during the last glacial maximum, *Nature* 372 (1994) 252–255.
- [29] D. Seidov, M. Sarnthein, K. Statterger, R. Prien, M. Weinelt, North Atlantic ocean circulation during the last glacial maximum and subsequent meltwater event: A numerical model, *J. Geophys. Res.* 101 (1996) 16305–16332.
- [30] A. Ganopolski, S. Rahmstorf, V. Petoukhov, M. Claussen, Simulation of modern and glacial climates with a coupled global model of intermediate complexity, *Nature* 391 (1998) 351–356.
- [31] D.W. Oppo, S.J. Lehman, Mid-depth circulation of the subpolar North Atlantic during the last glacial maximum, *Science* 259 (1993) 1148–1152.
- [32] N.C. Slowey, W.B. Curry, Enhanced ventilation of the North Atlantic subtropical gyre thermocline during the last glaciation, *Nature* 358 (1992) 665–668.
- [33] M. Sarnthein, E. Jansen, M. Weinelt, M. Arnold, J.-C. Duplessy, H. Erlenkeuser, A. Flatoey, G. Johannessen, T. Johannessen, S. Jung, N. Koc, L. Labeyrie, M. Maslin, U. Pflaumann, H. Schulz, Variations in Atlantic surface ocean paleoceanography, 50°–80°N: A time-slice record of the last 30,000 years, *Paleoceanography* 10 (1995) 1063–1094.
- [34] M. Weinelt, M. Sarnthein, U. Pflaumann, H. Schulz, S. Jung, H. Erlenkeuser, Ice-free Nordic Seas during the last glacial maximum? Potential sites of deepwater formation, *Paleoclim. Data Modell.* 1 (1996) 283–309.
- [35] E. Michel, L. Labeyrie, J.-C. Duplessy, N. Gorfti, M. Labracherie, J.L. Turon, Could deep Subantarctic convection feed the world deep basins during the last glacial maximum?, *Paleoceanography* 10 (1995) 927–942.
- [36] A.E. Gill, Circulation and bottom water production in the Weddell Sea, *Deep Sea Res.* 20 (1973) 111–140.
- [37] N.J. Shackleton, J.-C. Duplessy, M. Arnold, P. Maurice, M.A. Hall, J. Cartledge, Radiocarbon age of the last glacial Pacific deep water, *Nature* 335 (1988) 708–711.
- [38] W.S. Broecker, An oceanographic explanation for the apparent carbon isotope-cadmium discordancy in the glacial Antarctic?, *Paleoceanography* 8 (1993) 137–139.